The Journal of Neuroscience, May 1992, 12(5): 1781–1788

# Voltage-activated $K^+$ Currents in Acutely Isolated Hippocampal Astrocytes

**Frederick W. Tse,[a] Douglas D. Fraser, Steven Duffy, and Brian A. MacVicar**

Neuroscience Research Group, University of Calgary, Calgary, Alberta, Canada, T2N 4N1

**Hippocampal astrocytes were acutely isolated by papain treatment and mechanical trituration. Astrocytes were identified by their distinctive stellate morphology and immunocytochemical staining for glial fibrillary acidic protein. The electrophysiological properties of these cells were investigated using whole-cell voltage-clamp techniques. Three kinetically and pharmacologically distinct voltage-activated $K^+$ currents were identified in most cells; they resembled the neuronal A-current, delayed rectifier, and inward rectifier. The activation threshold of the A-current was −40 mV with a time to peak that ranged from 10 msec at −20 mV to 6 msec at 100 mV. Steady-state inactivation was observed when the holding potential was positive to −100 mV. The current was half-inactivated at −60 mV and totally inactivated at −20 mV. The A-current was suppressed by 4-aminopyridine (4-AP). The delayed rectifier was activated by depolarizing pulses more positive than −40 mV and had a half time of activation that ranged from 18 msec at −20 mV to 10 msec at potentials more positive than 40 mV. This current did not inactivate during a 100 msec pulse and was suppressed by extracellular tetraethylammonium (TEA). An inwardly rectifying current was elicited by hyperpolarizing pulses more negative than −80 mV. This current was not blocked by extracellular TEA or 4-AP and was never observed in the presence of external $Ba^{2+}$. Voltage-activated inward $Na^+$ currents were never observed. Voltage-activated $K^+$ channels may enhance the local $K^+$ spatial buffering capabilities of the astrocyte syncytium when extracellular $[K^+]$ increases during neuronal activity.**

Electrophysiological studies on astrocytes in primary cell culture have indicated that astrocytes express a variety of voltage-gated ionic channels (reviewed by Barres et al., 1990a). Two types of voltage-gated outward $K^+$ currents have been reported: a rapidly inactivating A-type current depressed by 4-aminopyridine (4-AP), and a noninactivating delayed rectifier depressed by tetraethylammonium (TEA) (Bevan and Raff, 1985; Bevan et al., 1985, 1987; Nowak et al., 1987). There is also evidence for an inwardly rectifying $K^+$ channel in cultured mouse astrocytes that was depressed by $Ba^{2+}$ (Nowak et al., 1987; Walz and Hinks, 1987). Both T- and L-type $Ca^{2+}$ currents have been reported, the latter has been shown to be modulated by cAMP and dihydropyridines (MacVicar, 1984; MacVicar and Tse, 1988; Barres et al., 1989a). Two types of $Cl^-$-selective channels have also been reported, a large-conductance channel opened by depolarization (Bevan et al., 1985, 1987; Gray and Ritchie, 1986; Nowak et al., 1987; Sonnhof, 1987), and an inwardly rectifying, small-conductance channel that is opened by hyperpolarization (Nowak et al., 1987). The former is depressed by the disulphonate stilbenes DIDS and SITS (Gray and Ritchie, 1986). A voltage-activated $Na^+$ channel has been identified in cultured astrocytes. The kinetic and pharmacological properties were similar to neuronal $Na^+$ channels except for a higher $K_d$ for block by TTX (Bevan et al., 1985, 1987; Nowak et al., 1987; Yarowsky and Krueger, 1989) and a steady-state inactivation curve that was shifted to more negative potentials (Sontheimer et al., 1991a).

Electrophysiological studies on astrocytes *in vivo* or in isolated brain slices have been limited because these cells form an electrotonically coupled network whose membrane potential cannot be uniformly controlled by conventional microelectrodes (e.g., Barres et al., 1990a; Burnard et al., 1990). It is not known if the expression of voltage-activated ionic channels in primary cultured astrocytes parallels ionic channel phenotype *in vivo*. For example, $Na^+$ current expression is altered during development of astrocytes in cell culture and is not observed in coupled astrocytes (Sontheimer et al., 1991a,b). Because culture conditions could induce novel expression of ion channels not normally expressed *in vivo*, enzymatic dissociation techniques have been recently developed for fast and reliable isolation of mature cells. Dissociation techniques have been utilized to investigate the electrophysiological properties of several vertebrate glia including Schwann cells (Chui, 1987; Wilson and Chui, 1989), retinal Müller cells (Newman, 1985; Brew et al., 1986; Nilius and Reichenbach, 1988), ependymal cells (Barres et al., 1989b), and O-2A progenitors from optic nerve (Barres et al., 1990b). A further advantage of enzymatic digestion is a clean membrane surface required for the formation of gigaohm seals with patch-clamp microelectrodes. Whole-cell voltage-clamp techniques enable greater control of membrane voltage and the ability to manipulate the intracellular contents for more complete channel blockade.

We have developed a method to dissociate acutely gray matter astrocytes from the hippocampus in order to examine their ionic currents with whole-cell voltage-clamp. Our results indicate that hippocampal astrocytes possess three voltage-activated $K^+$ currents.

Received July 1, 1991; revised Dec. 6, 1991; accepted Dec. 17, 1991.

We thank Dr. S. Barnes for helpful comments on the manuscript. This work was supported by a grant from the Medical Research Council (MRC) of Canada. F.W.T. is an Alberta Heritage Foundation for Medical Research (AHFMR) postdoctoral fellow and B.A.M. is an AHFMR Scholar and an MRC Scientist.

Correspondence should be addressed to Brian A. MacVicar at the above address.

[a] Present address: Department of Physiology and Biophysics, SJ-40, University of Washington, Seattle, WA 98195.

## Materials and Methods

*Acute dissociation.* Hippocampal astrocytes were isolated using a technique similar to those previously used to dissociate neurons (Kay and Wong, 1986) or salamander glia (Newman, 1986). Transverse hippocampal slices (500 μm) were obtained from Sprague–Dawley rats (21–35 d postnatal). The slices were incubated for 1 hr in artificial cerebrospinal fluid (aCSF) containing (in mM) 124 NaCl, 5 KCl, 1.3 $MgCl_2$, 2 $CaCl_2$, 26 $NaHCO_3$, and 10 D-glucose (pH 7.35; ~280 mOsm) aerated with 95% $O_2$, 5% $CO_2$ at 22°C. Slices were then transferred to a spinner flask (Bellco Glass Corp.) with a magnetic stirrer filled with aCSF at 35°C containing either 24 U/ml of papain with 0.24 mg/ml of L-cysteine or 42 U/ml of papain without L-cysteine. The slices were stirred at a rate sufficient to buoy them up and 95% $O_2$, 5% $CO_2$ was introduced continuously. After 1 hr the slices were transferred to aCSF, washed several times, and incubated at room temperature until trituration. When needed, a slice was then transferred to HEPES-buffered Dulbecco's modified Eagle's medium (DMEM) containing 1 mM kynurenic acid and 0.1 mM leupeptin, a $Ca^{2+}$-activated protease inhibitor. The CA1 was isolated with razor cuts under a dissecting microscope, transferred to a test tube containing 1 ml of the modified DMEM, and dispersed by trituration with fire-polished Pasteur pipettes. The whole solution was then transferred to the recording perfusion chamber mounted on an inverted microscope (IM-35, Zeiss).

Astrocytes were allowed to settle on a poly-L-lysine–coated coverslip for 10 min before the DMEM was replaced by superfusion of aCSF (22°C) containing 40 mM sucrose (pH 7.35; ~320 mOsm). The recording solution was aerated with 95% $O_2$, 5% $CO_2$, and the rate of superfusion was adjusted to allow complete exchange of chamber solution within 60 sec. High-resistance gigaohm seals were obtained from selected astrocytes, the membrane ruptured with negative pressure, and the cell contents exchanged with the pipette-filling solution containing (in mM) 120 KF, 10 EGTA, and 15 HEPES (pH 7.2; ~260 mOsm).

*Electrophysiological recording.* Patch electrodes were pulled from 1.0 mm o.d. thin-walled glass (1B 100F, World Precision Instruments) in two stages on a Narishige puller (PP-83). Electrodes were filled with the intracellular solution (described above) and had a tip resistence of 5–10 MΩ when tested in recording solution. A +7 mV liquid junction potential was measured between the electrode and bath solution. However, we did not correct for this junction potential in presenting our results. Current recordings were obtained using a single-electrode voltage-clamp amplifier (Axopatch-1A, Axon Instruments) and filtered at 1 kHz. Data were digitized with the TL-1-40 analog–digital interface (Axon Instruments). Computer-generated voltage command paradigms and data analysis were performed using pCLAMP software (Axon Instruments) running on a PC-AT (IBM Corp.).

*Immunohistochemistry.* Isolated cells were immunohistochemically tested for the presence of glial fibrillary acidic protein (GFAP), an intermediate-filament protein specific to astrocytes. Cells were fixed for 20 min in 4% formaldehyde and phosphate buffer after plating onto poly-L-lysine–coated coverslips. Fixed cells were washed and treated with 0.02% Triton-X in phosphate-buffered saline for 30 min. Nonspecific staining was blocked by pretreatment with normal horse serum, and staining due to endogenous peroxidase was blocked by pretreatment with $H_2O_2$. The fixed cells were subsequently exposed to a monoclonal antibody for GFAP (1:200 in phosphate buffer). The antibody was visualized by the avidin–biotin complex method and a final diaminobenzidine reaction.

*Materials.* All inorganic salts were purchased from Fisher. Chemicals utilized were papain (Sigma, P-4762), L-cysteine (Sigma, C-1276), leupeptin (Sigma, L-2884), tetraethylammonium (Sigma, T-1013), 4-aminopyridine (Sigma, A-0152), SITS (BDH Chemicals Ltd), HEPES (Sigma, H-3375), EGTA (Sigma, E-4378), Lucifer yellow (LY; Sigma, L-0144), GFAP (Boehringer Mannheim), and vectastain ABC kit (Vector Labs). During recording, all chemicals superfused were added hyperosmotically to the recording solution from concentrated stocks except for TEA, which replaced $Na^+$ isoosmotically.

## Results

*Morphology of isolated astrocytes*

Three morphologically distinct cell types were observed following dissociation. One type clearly resembled CA1 pyramidal neurons in that the cells typically had pyramidal-shaped somata with one major apical dendrite (Kay and Wong, 1986). The second cell type resembled CA1 interneurons in that they were fusiform, being multipolar with several primary dendritic branches still attached (Fraser and MacVicar, 1991). The last cell type, astrocytes, were easily discerned by their smaller cell bodies (5–8 μm) and numerous stellate processes (Fig. 1*A*). When isolated cells were stained for GFAP, an astrocyte-specific cytoskeletal protein, cells with astrocyte morphology were GFAP positive, whereas neurons were GFAP negative (Fig. 1*C*). Therefore, astrocytes could be identified by morphological criteria alone.

It was possible that the extensive processes that appeared to be part of the astrocytes could be attached debris from the dissociation technique. To test the continuity of the processes with the soma, cells were filled with 0.3% LY by inclusion of the dye within the patch pipettes. Following rupture of the membrane with negative pressure, LY diffused to the finest processes within seconds, indicating that the processes were continuous with the cell body (Fig. 1*B*; $n = 5$ of 5).

*Electrophysiological recording*

Under whole-cell voltage clamp, with patch electrodes of comparable tip resistance, the capacitive transient currents recorded in astrocytes outlasted those in isolated pyramidal neurons (>10 msec vs. <1 msec for neurons) and appeared to decay with more than one exponential function. These observations suggest that there is considerable axial resistence in the fine processes of each astrocyte, which is likely to cause nonuniform voltage control. Nonisopotential dendritic processes could affect (1) the activation threshold for each current, (2) the voltage range and steepness factor of activation and inactivation curves, and (3) the time for activation and inactivation. Therefore the results in this report will provide a qualitative assessment of the kinetics of the currents and cannot be used to quantify the properties of the currents precisely. We also cannot exclude the possibility that astrocytes may also possess other currents that are exclusively located on the most distal regions of the processes.

Whole-cell voltage-clamp data presented here were selected from 27 cells that had input resistances in the range of 250 MΩ to 1 GΩ and resting membrane potentials more negative than −50 mV. Currents were also examined in another 21 cells that had resting potentials more positive than −50 mV and/or input resistances <200 MΩ but were not included for analysis of volt-

→

*Figure 1.* Morphology of astrocytes acutely isolated from the CA1 region of hippocampal slices. *A*, Following enzymatic treatment with papain and mechanical trituration, a subpopulation of cells exhibited the well-defined morphology of pyramidal neurons (*A1*). Other cells had the typical stellate morphology of astrocytes (*A2–A4*), from which whole-cell voltage-clamp recordings were obtained. *B*, The stellate processes of astrocytes were continuous with the cell body and not attached debris, demonstrated by inclusion of LY within the patch pipette. *B1*, The astrocyte is illustrated before recordings were obtained. *B2*, LY diffused throughout the distal processes within seconds after rupturing the high-resistance seal to gain access to the cell interior. A portion of the cell is obscured by the LY-containing pipette. *B3*, Internal dialysis with LY and fluorescence observation was deleterious to the cell and altered the morphology. *C*, Cells were immunohistochemically stained for GFAP, those with stellate morphology were always GFAP positive, indicating that they were astrocytes (*C1–C3*), whereas neurons were GFAP negative (*C4*).

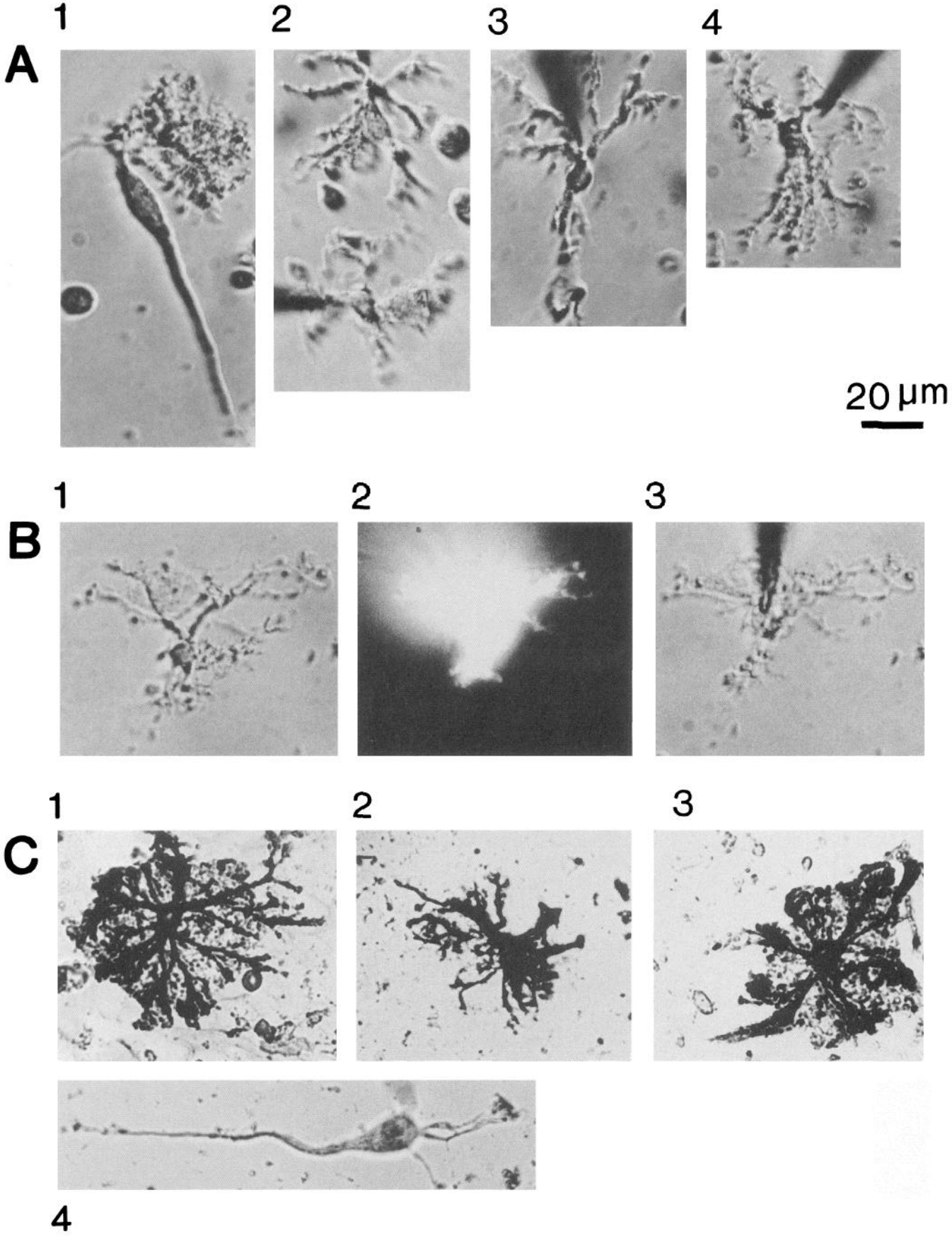
A
1
2
3
4
20 µm
B
1
2
3
C
1
2
3
4

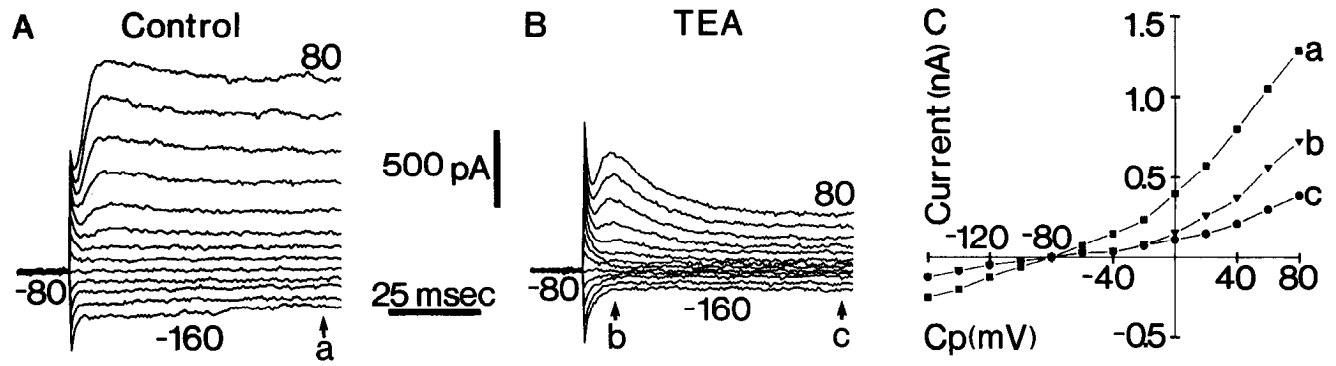


*Figure 2.* Transient and sustained outward currents in an acutely isolated astrocyte. *A*, Voltage command steps from −160 to 80 mV from a holding potential of −80 mV revealed an outward current that was observed with depolarization >−40 mV. Capacitive and leak currents were not subtracted. *B*, Superfusion of TEA (50 mM) blocked the sustained component of the outward current and a transient outward current was now observed. *C*, Plot of the *I/V* relationship of the outward currents illustrated in *A* and *B*. *Line a* was obtained in control solution at the time indicated by *arrow a* in *A*. In TEA the transient outward current became apparent (*arrow b, line b*) because the voltage-activated sustained outward current and leak current were suppressed (*line c, arrow c*).

age-activated currents because they were most likely damaged during the isolation procedure.

*A-current*

In 13 out of 15 cells, we observed a transient as well as a sustained component in the outward current when the cell was depolarized beyond −40 mV from a holding potential of −80 mV (Fig. 2). Application of 20–50 mM external TEA clearly depressed the sustained component but left the transient component unaffected. This TEA-insensitive transient component was reversibly inactivated at a holding potential of −40 mV (Fig. 3; $n = 13$). Subtraction of the currents obtained from a holding potential of −40 mV from those obtained at −80 mV revealed the transient component, without leak and capacitive current contamination. The transient outward current was selectively blocked by 1 mM 4-AP ($n = 6$) and was never observed when the electrode-filling solution contained 120 mM $Cs^+$ ($n = 12$), which has been shown to block outward $K^+$ currents.

The voltage dependence of steady-state inactivation and activation of the transient current is shown in Figure 4. Steady-state inactivation was measured by varying the holding potential from −100 mV to −20 mV and activating the current with a command potential to 60 mV. Steady-state inactivation was observed when the holding potential was positive to −100 mV. The current was half-inactivated at −60 mV and was totally inactivated at −20 mV. The fractional current, normalized to the maximum current, was smoothly voltage dependent and was fitted to the Boltzmann equation

$$I/I_{max} = \{1 + \exp[(V - V_{0.5})/k]\}^{-1},$$

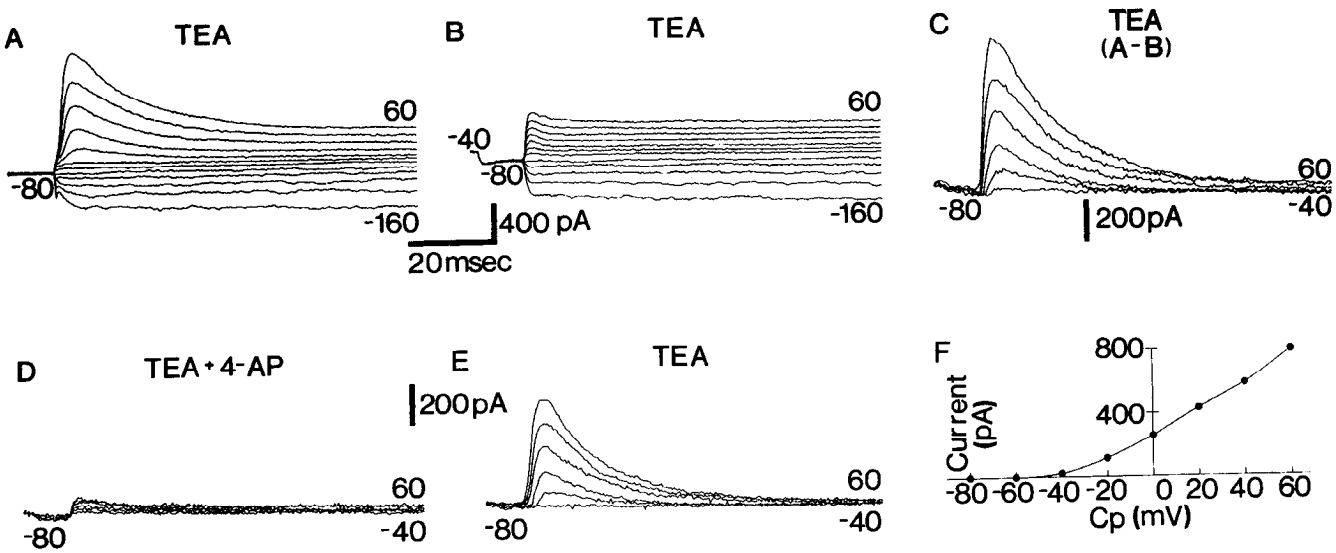


*Figure 3.* A voltage-activated $K^+$ current in astrocytes with kinetic and pharmacological properties similar to the neuronal A-current. *A*, Voltage command pulses from −160 to 60 mV from a holding potential of −80 mV revealed a TEA-insensitive outward current elicited by depolarization. *B*, The TEA-insensitive outward current was abolished when the cell was held at −40 mV. Cell membrane potential was stepped to −80 mV for 15 msec before applying the test pulses identical to *A*. *C*, Traces in *B* were subtracted from corresponding traces in *A* to reveal the TEA-insensitive transient current that was inactivated by a holding potential of −40 mV. *D*, The transient $K^+$ current, obtained using the same paradigm as in *C*, was blocked by 1 mM 4-AP. *E*, The transient $K^+$ current recovered following washout of the 4-AP. *F*, The current–voltage relationship of the TEA-insensitive transient current.

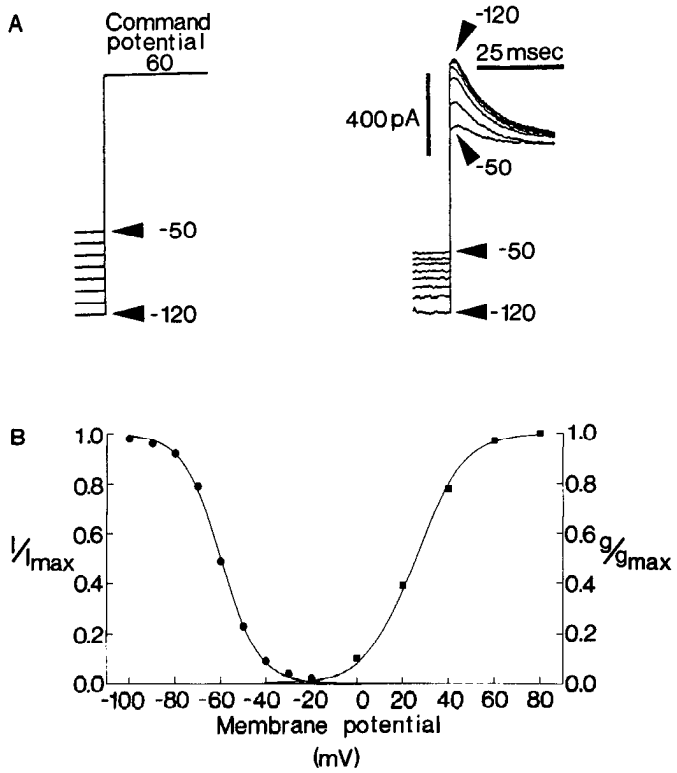


*Figure 4.* Steady-state inactivation and activation of the TEA-insensitive transient current. *A*, Steady-state inactivation of the current is illustrated by changing the holding potential from −120 to −50 mV for 5 sec and then evoking the current with a command potential to 60 mV. *B*, The inactivation curve (*left curve*) was investigated by changing the holding potential from −100 to −20 mV and evoking current by a command potential to 60 mV. The points were fitted by the first Boltzmann equation described in the Results. The voltage at which half-maximal inactivation occurred was −60 mV, and the steepness factor of the equation ($k$) was 6.3. The voltage-dependence of activation (*right curve*) was investigated by dividing the maximal current at each command potential, evoked from a holding potential of −80 mV, by ($V_C - E_K$). The points were fitted by the second Boltzmann equation described in the Results. The voltage at which half-maximal activation occurred was 25 mV, and the steepness factor of the equation ($k$) was 10.4.

where $I$ is peak current at the holding potential $V$, $I_{max}$ is the maximum current from a holding potential of −120 mV, $V$ is the holding potential, $V_{0.5}$ is the half-inactivation value, and $k$ is the steepness factor. The curve was best fit when $V_{0.5} = -60$ mV and $k = 6.3$. Steady-state activation was obtained by dividing the maximal inactivating current by the electrochemical driving force ($V_C - E_K$), where $V_C$ is the command potential

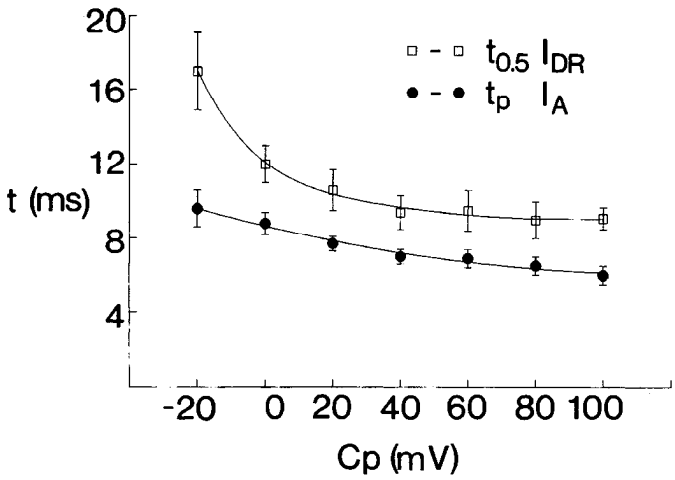


*Figure 6.* The voltage dependence of the time to peak ($t_p$) of the transient K⁺ current ($I_A$) and the time to half-activation ($t_{0.5}$) of the delayed rectifier ($I_{DR}$). The time to peak of the transient K⁺ current was voltage dependent and ranged from 10 msec at −20 mV command potential (*Cp*) to 6 msec at 100 mV (*Cp*). The time for half-activation of the $I_{DR}$ was slower illustrating its slower onset kinetics and ranged from 18 msec at −20 mV *Cp* to 10 msec at *Cp* > −40 mV. The points plotted are the mean ± SEM from eight cells for $I_A$ and five cells for $I_{DR}$.

and $E_K$ is the K⁺ equilibrium potential calculated from the Nernst equation. The conductance was half-maximally activated at 25 mV. The curve was smoothly voltage-dependent and was fit by the Boltzmann equation

$$g/g_{max} = \{1 + \exp[-(V - V_{0.5})/k]\}^{-1}.$$

The best fit of the curve was obtained when $V_{0.5} = 25$ mV and $k = 10.4$.

*Delayed rectifier*

The voltage-activated sustained current was isolated by either blocking the A-current with 1 mM 4-AP or by inactivating the A-current with a holding potential of −40 mV. With the latter strategy, currents were elicited by stepping to −80 mV from −40 mV 15 msec prior to evoking command voltage steps. Superfusion of 25–50 mM TEA reduced the voltage-activated sustained outward current ($n = 4$) (Fig. 5). Subtraction of the currents obtained in TEA from control currents revealed a TEA-sensitive sustained current that activated slowly following a short delay and had an activation threshold positive to −40 mV. This current was never observed when the electrode-filling solution contained 120 mM $Cs^+$ ($n = 12$).

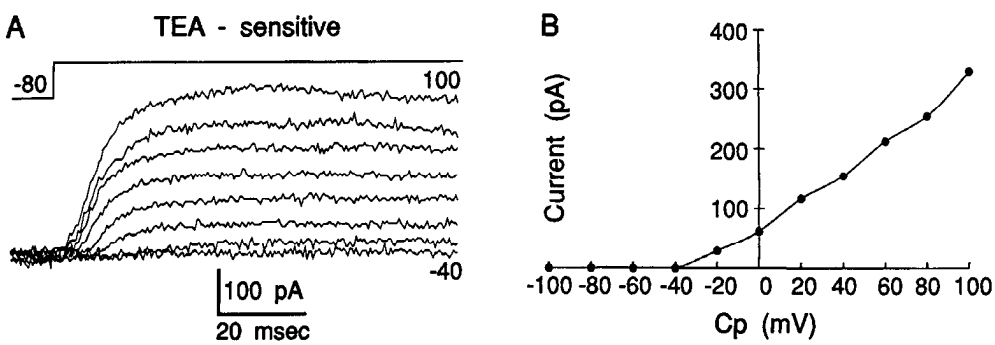


*Figure 5.* A voltage-activated K⁺ current in astrocytes with kinetic and pharmacological properties similar to the neuronal delayed rectifier. *A*, Voltage command pulses from −40 to 100 mV from a holding potential of −80 mV evoked an outward current that was blocked by superfusion of 50 mM TEA. The illustrated currents represent the TEA-sensitive component of the outward current. They were obtained by subtracting the leak and capacitative currents in TEA from the control currents. *B*, *I/V* plot of the TEA-sensitive currents illustrated in *A*.

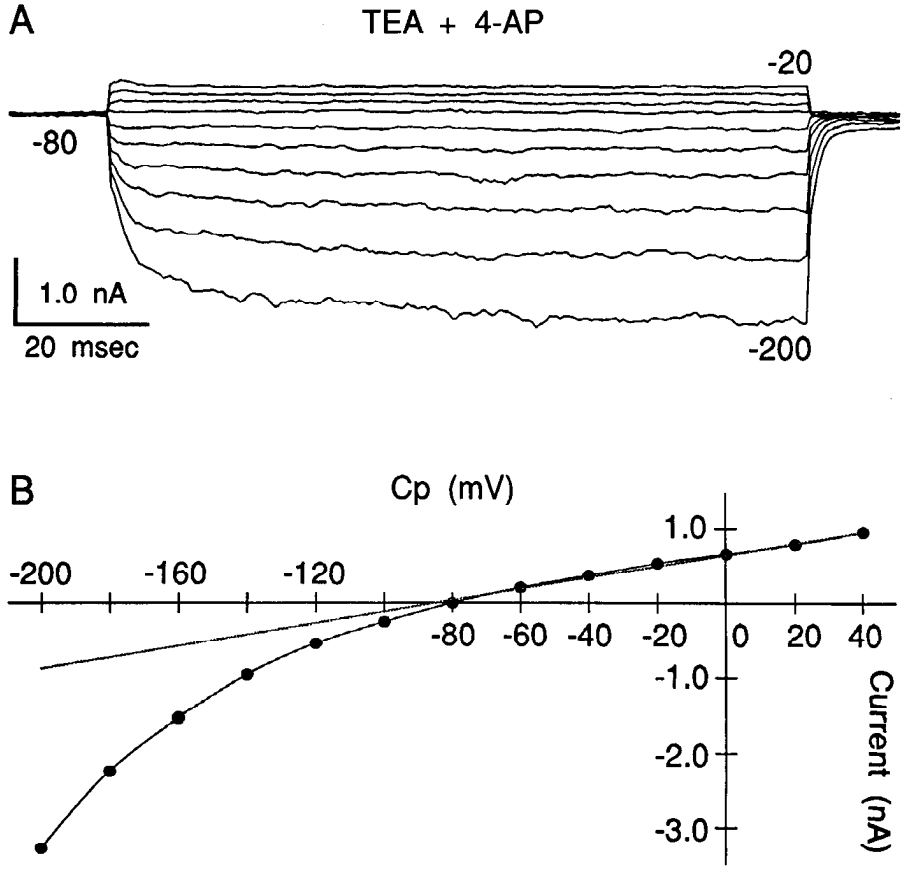


*Figure 7.* An inwardly rectifying current in acutely isolated astrocytes. *A*, The current was elicited with hyperpolarizing command potentials from a holding potential of −80 mV. The inward current was independent of extracellular TEA or 4-AP and never present when the external solution contained $Ba^{2+}$. The illustrated currents were not leak subtracted. *B*, The current–voltage relationship of the inward $K^+$ current (*solid line*) and the leak current (extrapolated *broken line*).

The time to half-activation of the delayed rectifier was voltage dependent and ranged from 18 msec at −20 mV to 10 msec at >40 mV (Fig. 6). Command voltage steps (<100 msec) did not cause inactivation of the delayed rectifier. In contrast, the time to peak ($t_p$) of the transient current was faster ranging from 10 msec at −20 mV to 6 msec at 100 mV (Fig. 6). The time to half-inactivation of the transient current was not strongly voltage dependent and was approximately 12 msec (not shown). Therefore, the A-current could activate and be significantly inactivated before peak activation of the delayed rectifier.

*Inward rectifier*

In all astrocytes, the current–voltage relationship revealed some degree of inward rectification at potentials negative to −80 mV (Fig. 7). The inward current increased gradually and did not reach a steady-state amplitude within the 100 msec command potentials. The current was not blocked by external TEA or 4-AP and was never observed in the presence of extracellular $Ba^{2+}$ (10 mM; $n = 3$), which blocks inwardly rectifying $K^+$ channels.

*Other ionic currents*

In the present study, even when the outward currents were blocked, either by internal $Cs^+$ or by external TEA and 4-AP, no voltage-activated inward $Na^+$ current was detected. Whole-cell voltage-clamp recordings from hippocampal neurons, prepared simultaneously with astrocytes, always revealed a $Na^+$ current of >2 nA (data not shown). There was also no indication of voltage-activated $Ca^{2+}$ channels, which was most likely due to the inclusion of $F^-$ in the pipette. $F^-$ is known to prevent the detection of some $Ca^{2+}$ current subtypes (Kay et al., 1986; Carbone and Lux, 1987). In other experiments, evidence from fura-2 and indo-1 fluorescence studies on acutely dissociated astrocytes indicates that depolarization induces an increase in $[Ca^{2+}]_i$ through voltage-activated $Ca^{2+}$ channels (Duffy et al., 1990).

In addition, we tested whether there were significant $Cl^-$- or $Ca^{2+}$-dependent $K^+$ currents in the astrocytes by applying either a blocker of voltage-activated $Cl^-$ channels, 100 μM SITS ($n = 3$) (Gray and Ritchie, 1986), or a blocker of $Ca^{2+}$ channels, 1 mM $Cd^{2+}$ or $Co^{2+}$. These blockers had no detectable effects on either the passive leakage current or the voltage-activated outward currents. However, in all experiments the recording pipette included 10 mM EGTA, a $Ca^{2+}$ ion chelator; therefore, the negative results with $Ca^{2+}$ channel blockers do not rule out the existence of $Ca^{2+}$-activated currents (e.g., Quandt and MacVicar, 1986).

## Discussion

Evidence from the present study demonstrates that acutely isolated astrocytes from the rat hippocampus express at least three of the voltage-activated $K^+$ channels that are present in cultured astrocytes. The delayed rectifier and A-current in acutely isolated cortical astrocytes resemble their counterpart in neurons and cultured astrocytes in terms of kinetics and pharmacology (Bevan et al., 1985, 1987; Nowak et al., 1987; Rudy, 1988). The voltage-activated inwardly rectifying channel in isolated astrocytes is open near resting membrane potential and appears similar to the inward rectifier previously described in central neurons (Constanti and Galvin, 1983; Williams et al., 1988a,b) and cardiac cells (Brown and Difrancesco, 1980; Noble, 1984). There

is evidence that this current is present in mouse astrocytes from primary culture (Nowak et al., 1987; Walz and Hinks, 1987), in acutely dissociated retinal Müller cells (Newman, 1985; Brew et al., 1986; Nilius and Reichenbach, 1988), and in O2A progenitor cells (Barres et al., 1990b). In contrast, microglia cells have an inwardly rectifying current that inactivates rapidly at negative potentials (Kettenmann et al., 1990).

Voltage-activated $Na^+$ channels were not observed in acutely dissociated cortical astrocytes, although such channels have been previously described in primary culture (Bevan et al., 1985, 1987; Nowak et al., 1987; Yarowsky and Krueger, 1989). It is unlikely that enzymatic digestion preferentially destroyed astrocyte $Na^+$ channels because neuronal $Na^+$ currents were still present in neurons co-isolated with the astrocytes. However, $Na^+$ channels in astrocytes could exist only on distal processes, which may not be observed during voltage-clamp of the cell body. Another possibility is that $Na^+$ channels are not expressed in the mature astrocyte *in vivo* but are only expressed during some stages of development. The kinetics of $Na^+$ currents change during development in cell culture (Sontheimer et al., 1991a) and $Na^+$ currents are not expressed in electrically coupled cultured astrocytes (Sontheimer et al., 1991b). These results stress the importance of examining ion channel expression in mature astrocytes that have not been cultured.

Both the A-type and delayed-rectifier $K^+$ currents had activation thresholds (−40 mV) that were significantly depolarized with respect to the normal resting potential of these cells (approximately −80 mV in 5 mM $K^+$; Burnard et al., 1990). However, if $K^+$ channels were located principally on the distal processes, then the axial resistance of the processes and electrotonic decay of the voltage command pulse would increase the apparent activation threshold. Therefore, our analysis of astrocyte $K^+$ currents is constrained by the physical dimensions of these cells. If the imperfect space clamp indeed shifted the apparent activation threshold to more depolarized potentials, then these currents could be activated near the normal resting potential.

The function of the three voltage-activated $K^+$ channels in astrocytes is speculative but could be related to $K^+$ homeostasis (Orkand et al., 1966; Walz and Hertz, 1983; Ballanyi et al., 1987). Extracellular $K^+$ is increased during neuronal activity. Astrocytes have been postulated to play an important role in buffering interstitial $K^+$ and limiting the extent of the increase. At present, two mechanisms, spatial buffering and $K^+$ accumulation, which are not mutually exclusive, have been proposed in which glia regulate the surrounding microenvironment via membrane permeability to $K^+$ (reviewed by Walz, 1989).

In the first mechanism, spatial buffering (Orkand et al., 1966), the high $K^+$ permeability of astrocytes would facilitate the flow of $K^+$ from an area of high concentration to areas of low concentration through the astrocyte network. Because $K^+$ would be carried by passive electrotonic current spread, spatial buffering would occur if the increases in external $K^+$ were localized to areas that were smaller than the electrotonic length of the network. The presence of voltage-activated $K^+$ channels could dynamically regulate the spatial buffering capabilities of the astrocyte network both by changing $K^+$ permeability at the site of increased external $K^+$ and by altering passive current spread. A modification of the spatial buffering theory, termed $K^+$ siphoning, has been suggested to occur in the retina where the direction of the $K^+$ shunt is dictated by regional distribution of $K^+$ conductances, particularly the inward rectifier (Newman et al., 1989). The presence of inwardly rectifying channels in acutely isolated astrocytes suggests that the $K^+$ siphoning may also occur in the hippocampus.

Rapid increases in extracellular $K^+$, observed during interictal spiking (reviewed by Dichter and Ayala, 1987), would transiently depolarize astrocytes and possibly activate the A-type $K^+$ channel (which activates in <10 msec), whereas prolonged extracellular $K^+$ increases during seizures (reviewed by Heinemann and Lux, 1983) or theta activity (MacVicar and Tse, 1989) would also activate the delayed-rectifier-type $K^+$ channel (which activates in >10 msec). The permeability of $K^+$ through the astrocyte membrane would thereby be increased, and consequently a greater proportion of $K^+$ would diffuse into the astrocyte to be dispersed by the surrounding astrocyte syncytium.

The second mechanism by which $K^+$ homeostasis could be maintained is by intracellular $K^+$ accumulation. It has been proposed that $K^+$ is sequestered into astrocytes in areas of high extracellular $K^+$ as a result of KCl accumulation due to Na–K–2Cl cotransport (Walz, 1989). In experiments utilizing optical imaging of hippocampal slices (MacVicar and Hochman, 1991), we have evidence for activity-induced cellular swelling that was sensitive to furosemide, an Na–K–2Cl cotransport inhibitor (Walz and Hertz, 1984; Kimelberg and Frangakis, 1985). It is possible that the swelling was due to Na–K–2Cl cotransport and osmotically induced water uptake into astrocytes. This has been shown to occur in astrocytes in cell culture (Walz, 1987; Walz and Mukeji, 1988) and in the rat optic nerve (Ransom et al., 1985). Alternatively, $K^+$ influx may passively follow an influx of $Cl^-$ through voltage-activated $Cl^-$ channels that open in response to depolarization (Bevan et al., 1985; Ballanyi et al., 1987). A passive uptake of KCl is possible if inwardly rectifying $K^+$ channels are present and open at the resting membrane potential. However, to maintain electroneutrality, a proportional inward $Cl^-$ conductance must also exist (Boyle and Conway, 1941). Experiments using intracellular recordings from astrocytes in hippocampal slices have not demonstrated any significant $Cl^-$ permeability of these cells at rest (MacVicar et al., 1989) and the reversal potential for $Cl^-$ in astrocytes appears to be such that an efflux of $Cl^-$ occurs at the resting membrane potential (Ballanyi et al., 1987; Kettenmann et al., 1988; MacVicar et al., 1989). In this study, a voltage-gated $Cl^-$ channel was not observed in acutely isolated hippocampal astrocytes, although it has been demonstrated in culture (Bevan et al., 1985). $K^+$ accumulation into astrocytes could be an important regulator of ionic homeostasis in the CNS, but if it occurs it is most likely due to transport mechanisms.

The results in this article represent the first ion channel analysis of astrocytes acutely isolated from a cortical region. The presence of voltage-activated $K^+$ channels could indicate that the interstitial $K^+$ buffering capabilities by astrocytes are increased by depolarization.

## References

Ballanyi K, Grafe P, Ten Bruggencate G (1987) Ion activities and potassium uptake mechanisms of glial cells in guinea-pig olfactory cortex slices. J Physiol 382:159–174.

Barres BA, Chun LLY, Corey DP (1989a) Calcium current in cortical astrocytes: induction by cAMP and neurotransmitters and permissive effect of serum factors. J Neuroci 9:3169–3175.

Barres BA, Chun LLY, Corey DP (1989b) Glial and neuronal forms of the voltage-dependent sodium channel: characteristics and cell-type distribution. Neuron 2:1375–1388.

Barres BA, Chun LLY, Corey DP (1990a) Ion channels in vertebrate glia. Annu Rev Neurosci 13:441–474.

Barres BA, Koroshetz WJ, Swartz KJ, Chun LLY, Corey DP (1990b)

Ion channel expression by white matter glia: the O-2A glial progenitor cell. Neuron 4:507–524.
Bevan S, Raff M (1985) Voltage-dependent potassium currents in cultured astrocytes. Nature 315:229–232.
Bevan S, Chiu SY, Gray PTA, Ritchie JM (1985) The presence of voltage-gated sodium, potassium and chloride channels in rat cultured astrocytes. Proc R Soc Lond [Biol] 225:299–313.
Bevan S, Lindsay RM, Perkins MN, Raff MC (1987) Voltage-gated ionic channels in rat cultured astrocytes, reactive astrocytes, and an astrocyte-oligodendrocyte progenitor cell. J Physiol (Lond) 82:327–335.
Boyle PJ, Conway EJ (1941) Potassium accumulation in muscle and associated changes. J Physiol (Lond) 100:1–63.
Brew H, Gray PTA, Mobbs P, Attwell D (1986) Endfeet of retinal glial cells have higher densities of ion channels that mediate potassium buffering. Nature 324:466–468.
Brown H, Difrancesco D (1980) Voltage-clamp investigations of membrane currents underlying pacemaker activity in rabbit sino-atrial node. J Physiol (Lond) 308:331–351.
Burnard DM, Crichton SA, MacVicar BA (1990) Electrophysiological properties of reactive glial cells in kainate-lesioned hippocampal slice. Brain Res 510:43–52.
Carbone E, Lux HD (1987) Kinetics and selectivity of a low voltage-activated calcium current in chick and rat sensory neurons. J Physiol (Lond) 386:547–570.
Chui SY (1987) Sodium currents in axon-associated Schwann cells from adult rabbits. J Physiol (Lond) 386:181–203.
Constanti A, Galvin M (1983) Fast inward-rectifying current accounts for anomalous rectification in olfactory cortex neurons. J Physiol (Lond) 385:153–178.
Dichter MA, Ayala GF (1987) Cellular mechanisms of epilepsy: a status report. Science 237:157–164.
Duffy S, Tse FW, Hochman D, Fraser DD, MacVicar BA (1990) Voltage-activated $K^+$ and $Ca^{++}$ channels in acutely isolated hippocampal astrocytes. Soc Neurosci Abstr 16:666.
Fraser DD, MacVicar BA (1991) Low-threshold transient calcium current in rat hippocampal lacunosum-moleculare interneurons: kinetics and modulation by neurotransmitters. J Neurosci 11:2812–2820.
Gray PTA, Ritchie JM (1986) A voltage-gated chloride conductance in rat cultured astrocytes. Proc R Soc Lond [Biol] 228:267–288.
Heinemann U, Lux HD (1983) Ionic changes during experimentally induced epilepsies. In: Research progress in epilepsy (Rose C, ed), pp 87–103. New York: Pitman.
Kay A, Wong RKS (1986) Isolation of neurons suitable for patch-clamping from adult mammalian central nervous system. J Neurosci Methods 16:227–238.
Kay A, Miles R, Wong RKS (1986) Intracellular fluoride alters the kinetic properties of calcium currents facilitating the investigation of synaptic events in hippocampal neurons. J Neurosci 6:2915–2920.
Kettenmann H, Backus KH, Schachner M (1988) GABA receptors on cultured astrocytes. In: Glial cell receptors (Kimelberg HK, ed), pp 95–106. New York: Raven.
Kettenmann H, Hoppe D, Gottmann K, Banati R, Kreutzberg G (1990) Cultured microglial cells have a distinct pattern of membrane channels different from peritoneal macrophages. J Neurosci Res 26:278–287.
Kimelberg HK, Frangakis MV (1985) Furosemide- and butenamide-sensitive ion transport and volume control in primary astrocyte cultures from rat brain. Brain Res 61:125–134.
MacVicar BA (1984) Voltage-dependent calcium channels in glial cells. Science 226:1345–1347.
MacVicar BA, Hochman D (1991) Imaging of synaptically evoked intrinsic optical signals in hippocampal slices. J Neurosci 11:1458–1469.
MacVicar BA, Tse FW (1988) Norepinephrine and cyclic adenosine 3′:5′-cyclic monophosphate enhance a nifedipine-sensitive calcium current in cultured rat astrocytes. Glia 1:359–365.
MacVicar BA, Tse FW (1989) Local neuronal circuitry underlying cholinergic rhythmical slow activity in CA3 region of rat hippocampal slices. J Physiol (Lond) 417:197–212.
MacVicar BA, Tse FW, Crichton SA, Kettenmann H (1989) GABA-activated chloride channels in astrocytes of hippocampal slices. J Neurosci 9:3577–3583.
Newman EA (1985) Voltage-dependent calcium and potassium channels in retinal glial cells. Nature 317:809–811.
Newman EA (1986) High potassium conductance in astrocyte endfoot. Science 233:453–454.
Newman EA, Frambach DA, Odette LL (1989) Control of extracellular potassium levels by retinal glial cell potassium siphoning. Science 225:1174–1175.
Nilius B, Reichenbach A (1988) Efficient potassium buffering by mammalian retinal glial cells is due to cooperation of specialized ion channels. Pfluegers Arch 411:654–660.
Noble D (1984) The surprising heart: a review of recent progress in cardiac electrophysiology. J Physiol (Lond) 353:1–50.
Nowak L, Ascher P, Berwald-Netter Y (1987) Ionic channels in mouse astrocytes in culture. J Neurosci 7:101–109.
Orkand RK, Nicholls JG, Kuffler SW (1966) Effect of nerve impulses on the membrane potential of glial cells in the central nervous system of amphibia. J Neurophysiol 29:788–806.
Quandt FM, MacVicar BA (1986) Calcium-activated potassium channels in cultured astrocytes. Neuroscience 19:29–41.
Ransom BR, Yamate CL, Connors BW (1985) Activity-dependent shrinkage of extracellular space in rat optic nerve: a developmental study. J Neurosci 5:532–535.
Rudy B (1988) Diversity and ubiquity of potassium channels. Neuroscience 25:729–749.
Sonnhof U (1987) Single voltage-dependent potassium and chloride channels in cultured rat astrocytes. Can J Physiol Pharmacol 65:1043–1050.
Sontheimer H, Ransom BR, Cornell-Bell AH, Black JA, Waxman SG (1991a) $Na^+$-current expression in rat hippocampal astrocytes *in vitro*: alterations during development. J Neurophysiol 65:3–19.
Sontheimer H, Waxman SG, Ransom BR (1991b) Relationship between $Na^+$ current expression and cell–cell coupling in astrocytes cultured from rat hippocampus. J Neurophysiol 65:989–1002.
Walz W (1987) Swelling and potassium uptake in cultured astrocytes. Can J Physiol Pharmacol 65:1051–1057.
Walz W (1989) Role of glial cells in the regulation of the brain ion microenvironment. Prog Neurobiol 33:309–333.
Walz W, Hertz L (1983) Functional interactions between neurons and astrocytes. 2. Potassium homeostasis at the cellular level. Prog Neurobiol 20:133–183.
Walz W, Hertz L (1984) Intense furosemide-sensitive potassium accumulation in astrocytes in the presence of pathologically high extracellular potassium levels. J Cereb Blood Flow Metab 4Z:301–304.
Walz W, Hinks EC (1987) Extracellular hydrogen ions influence channel-mediated and carrier-mediated potassium fluxes in cultured mouse astrocytes. Neuroscience 20:341–346.
Walz W, Mukeji S (1988) KCl movements during potassium-induced cytotoxic swelling of cultured astrocytes. Exp Neurol 99:17–29.
Williams JT, Colmers WF, Pan ZZ (1988a) Voltage- and ligand-activated inwardly rectifying currents in dorsal raphe neurons *in vitro*. J Neurosci 8:3499–3506.
Williams JT, North RA, Tokimasa T (1988b) Inward rectification of resting and opiate-activated potassium currents in rat locus coeruleus neurons. J Neurosci 8:4299–4306.
Wilson GF, Chui SY (1989) Regulation of Schwann cell potassium channels during initial stages of myelinogenesis. Soc Neurosci Abstr 15:993.
Yarowsky PJ, Krueger BK (1989) Development of saxitoxin-sensitive and insensitive sodium channels in cultured neonatal rat astrocytes. J Neurosci 9:1055–1061.